

Orbital Decay of Low Earth Orbit Satellites: A Numerical Investigation

Md Ajim Hossain

M.Sc. Student, Dept. of Physics, Barasat Govt. College, WBSU, Barasat, West Bengal, India

Abstract— Now a days the number of earth satellites orbiting in Low Earth Orbit (LEO) is increasing day by day. Low Earth Orbit (LEO) satellites play very crucial role in various spaced-based applications: such as communication, scientific researches and other important sectors, but they experience natural decay of their orbits due to atmospheric drag and other influencing factors. For low altitude, the air density is large enough which leads atmospheric drag to become the major influencing factor for orbital decay of LEO satellites. Investigating and predicting this decay is essential for satellite operators to optimize their mission duration and avoid space debris. In this paper, we shall present a numerical investigation of LEO satellite orbital decay using Python language employing 4th order Runge Kutta method in presence of quadratic drag. We shall investigate the decay behavior, life time duration and other relevant interesting parameters. Finally, we shall validate our numerical results against experimental data. This validation process will ensure us that our numerical model is accurate enough to estimate the real world orbital decay behavior of LEO satellites.

Keywords— Atmospheric drag, Low Earth Orbit, LEO satellite.

I. INTRODUCTION

In this section, we discuss about the significance of the numerical investigation of orbital decay of LEO satellites as well as our primary objectives to this study. We shall also provide a road map of this paper outlining the main sections including the basic theoretical idea, mathematical formulations, result analysis, validations against experimental data and model visualization as well.

I.A Background and Motivation

The number of satellites sent into space is increasing day by day. Upon launch, a satellite is placed in one of the particular orbits around the Earth or it is to be sent on an interplanetary journey i.e. its journey to a final destination like Mars or Jupiter or may be Moon. Followings are several types of orbits of satellite on the basis of orbital altitude (i.e. distance from Earth's surface):

- Low Earth Orbit (LEO)
- Medium Earth Orbit (MEO)
- Geostationary Orbit (GEO)
- Sun Synchronous Orbit (SSO)

Low Earth Orbit satellites are moving at an altitude of roughly 160-1600 kilometres above the Earth surface. They typically take time between 90 to 120 minutes to complete one full orbit. They are commonly used for remote sensing, high-resolution Earth observation and scientific researches as well. LEO is also used for the International Space Station (ISS) and Hubble Telescope.

Medium Earth Orbit is located at an altitude above LEO and below GEO in between 2000 and 35786 kilometres above the Earth surface. Satellites in MEO have an orbital period ranging between 2 and 24 hours. MEO is commonly used for navigation systems including Global Positioning System (GPS).

Geostationary Orbit (GEO) satellites are moving around the Earth above the equator from west to east following the Earth's rotation having a period of 23 hours 56 minutes 4 seconds. They

are placed at an altitude of 35786 kilometres directly above the equator. They appear at a fixed position in the sky band are used for telecommunications and earth observations.

Sun Synchronous Orbit (SSO) is a special type of polar orbit. Satellites in SSO are synchronised to be in the fixed position relative to the Sun. They are orbiting in such a way that they pass over an Earth region at the same local time every day.

In recent years, there has been a significant increase in the number of satellites in space. A satellite tracking website *orbiting-now.com* lists almost 7,702 active satellites in various Earth orbits. This data is recorded as of 4th may, 2023. However, the increasing number of satellites poses a set of challenges: particularly related to orbital decay i.e. a gradual decrease in altitude.

There are many factors such as atmospheric drag, gravity field irregularities, solar radiation pressure and the electromagnetic effects which absorb energy from orbital motion and thereby cause of orbital decay. For satellites in LEO, atmospheric drag is major significant factor causing orbital decay. About 90% of all satellites are orbiting in LEO. And we are also interested to study this LEO satellites orbital decay.

There are some key reasons and importance to study orbital decay whose are briefly discussed below.

(a) Space Mission Planning: Satellites are designed for specific space mission planning. Predictions of orbital decay enable the space mission planners to determine an accurate lifetime of satellite. With the knowledge of orbital decay rates, the space mission planners can optimize the operational life span and efficiently improve functionality of satellites for which they are intended.

(b) Satellite Operations: Precise knowledge about orbital decay is significant for satellite operators to manage the operation and control of their satellites. This is the vital information for satellite operators to take important decisions to maintain safe and efficient satellite operations and reduce risk of collisions with other operational satellites or space debris.

(c) Space Debris Management: Timely and accurate estimation of orbital decay is crucial for managing space debris and reducing the accumulation of debris in space.

I.B Research Objectives

The main objectives for developing this work on the numerical investigation of LEO satellites are discussed below.

(a) Understanding mechanics behind orbital decay: Our primary objective of this work is to understand the theoretical background related to the orbital mechanics incorporating the factors influencing the decay process. We consider only the atmospheric drag effect as it is major influencing factor for Low Earth Orbit.

(b) To develop a numerical model: We shall develop a numerical model to simulate & predict the orbital decay of LEO satellites over time. This model will be capable for various satellite configurations and decay factors. We shall develop a Python code to simulate this model.

(c) Numerical data analysis: Numerical data analysis enables the assessment of the decay rate of LEO satellites. We shall calculate various orbital decay parameters and analyse them to gain insights into the factors driving orbital decay and their respective contributions to the decay rate.

(d) Validation of the model against experimental data: It is essential to validate our numerical data against experimentally obtained data for ensuring the accuracy and reliability of our numerical model. In this paper, we shall also perform a numerical calculation for ISS and Tiangong-1 satellite for validation purposes.

I.C Paper Outlines

In section II we discuss about the dynamics behind orbital motion of satellite. Under section II, in subsection II.A we describe two body central force problem: equivalent one body problem and Kepler's laws of planetary motion. Whereas subsection II.B deals with atmospheric density variation at different altitudes and quadratic nature of atmospheric drag. In subsection II.C we present mathematical formulation of orbital decay model. Subsection II.D outlines an analytical approach to calculate decay rate. In Section III we present our numerically obtained results and their analysis as well as validation against experimental data. Under section III, subsection III.A presents a primary model validation approach. In subsection III.B we present numerically calculated data in tabulated forms as well as analyze them graphically. Subsection III.C validates the numerical model against ISS orbital decay data and Tiangong-1 reentry data. In section IV we present 3D visualization of orbital decay model. And section V draws a conclusion.

II. SATELLITE ORBITAL DYNAMICS & ATMOSPHERIC DRAG EFFECT

To develop an accurate numerical model of orbital decay of LEO satellites, it is essential to understand the orbital dynamics of satellite motion and the effects of atmospheric drag. In this section, we focus on satellite orbital dynamics and atmospheric drag effects in the context of orbital decay.

II.A Satellite Orbital Motion

In this subsection, we discuss about the key concepts and governing principles of satellite orbital motion. This is very

crucial for accurate modeling the orbital decay of LEO satellites.

(a) Two body central force problem:

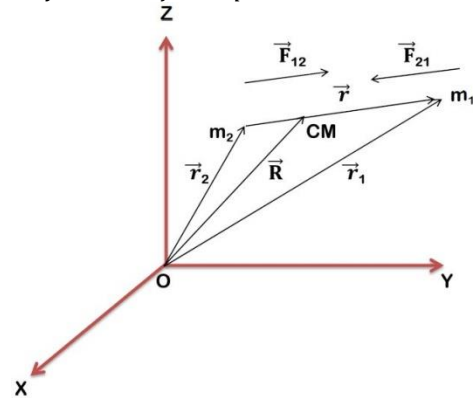


Fig 1: Representation of Two body system.

Let us consider two objects of masses m_1 and m_2 , whose position vectors with respect to the origin O of some inertial frame of reference are denoted as \vec{r}_1 and \vec{r}_2 respectively. In case of two astronomical bodies (Earth & satellite for instance) the force acting between them is gravitational force. We neglect here the influences of other celestial bodies. The force exerted by the object of mass m_2 on object of mass m_1 is expressed as

$$\vec{F}_{12} = \frac{Gm_1m_2}{|\vec{r}_1 - \vec{r}_2|^2} \hat{r} \tag{1}$$

And force on the object of mass m_2 due to the object of mass m_1 is given by

$$\vec{F}_{21} = -\frac{Gm_1m_2}{|\vec{r}_1 - \vec{r}_2|^2} \hat{r} \tag{2}$$

Here, \hat{r} is the unit vector along the line joining the two objects, $\hat{r} = \frac{\vec{r}_1 - \vec{r}_2}{|\vec{r}_1 - \vec{r}_2|}$. For simplification, we can reduce this into an equivalent one body problem by incorporating the concept of reduced mass. Let us define the reduced mass, $\mu = \frac{m_1m_2}{m_1 + m_2}$. By introducing the reduced mass following some calculations we obtain equation of motion for reduced one body problem as:

$$\mu \frac{d^2\vec{r}}{dt^2} = -\frac{Gm_1m_2}{r^2} \hat{r} \tag{3}$$

In this reduced problem, we can assume a single point mass μ moving under the influence of a central force. In our Earth-satellite problem, mass of satellite is significantly very less compared to that of Earth. Let say, mass of Earth and satellite be denoted as M and m_s respectively.

Using $m_s \ll M$ condition equation-3 further reduces to

$$\frac{d^2\vec{r}}{dt^2} = -\frac{GM}{r^2} \hat{r} \tag{4}$$

As we know, the value of gravitational constant G cannot be measured with high accuracy. For this reason we use standard gravitational parameter GM whose value is taken as $3.986004418 \times 10^{14} m^3s^{-2}$. The equation-4 indicates that the satellite's acceleration is solely determined by the gravitational force which is exerted by the Earth.

(b) Keplers laws of planetary motion:

This part explores the Kepler's laws and their relevance to satellite orbits. These are applicable to satellite orbits.

Law of Ellipses: According to this law, the orbit of satellite is an ellipse with the central body (Earth) located at one of ellipse's

foci. The shape of the orbit is determined by the eccentricity of the ellipse. The orbit is circular for eccentricity, $e = 0$ and elliptical for eccentricity, $e > 0$. In our case of LEO satellites, we assume that the orbit is circular i.e. $e = 0$.

Law of Equal areas: This law relates that a line segment joining the satellite to the central body (in our case: Earth) sweeps out equal areas during equal intervals of time. This means, a satellite moves faster during its position is closer the Earth and slower when it is far away from the Earth. Satellite's orbital velocity varies throughout its orbits.

Law of Harmonics: This law states that the square of a satellite's orbital period is proportional to the cube of the length of the semi-major axis of its orbit. This implies square of the Time Period (T):

$$T^2 = \left(\frac{4\pi}{GM}\right) a^3, \quad (5)$$

where a and GM be the length of semi-major axis and standard gravitational parameter of the Earth respectively.

These laws enable us for accurately modelling the orbital decay of LEO satellites with gravitational force exerted by the Earth in presence of atmospheric drag effects. In the next subsection we shall discuss about these effects.

II.B Atmospheric Drag Effects

This subsection deals with theory and mathematical formulations of atmospheric drag effects on satellite motion. When satellite moves within the Earth's atmosphere, it faces a resistance force which opposes the satellite motion. This force is due to the interactions between atmospheric molecules and satellite's surface area exposed to the airflow. This interaction is collision under molecular level through momentum transfer between atmospheric molecules and satellite. Individual collision does not cause any significant effect rather the overall effects of numerous collisions over time contribute to decelerate the satellite motion. Understanding this atmospheric effect is crucial for predicting the decay nature of satellite orbit.

(a) Atmospheric density:

In study of LEO satellites orbital decay, it is important to know the variation of atmospheric density at different altitudes. The atmospheric density generally decreases exponentially with increasing altitude. Depending upon some factors such as location, time of year, weather condition and other atmospheric phenomena atmospheric density can deviate from mean values. To simulate our numerical model the value of atmospheric density is needed at any altitude for every moment of time during simulation. There are many atmospheric models available for variation of air density with altitude. Out of them one most commonly used model is Mass Spectrometer Incoherent Scatter (MSISE-90) model of Earth's upper atmosphere [1]. It is based on mass spectrometer data from various satellites. We shall use this data to simulate our model for predicting satellite lifetime.

There are some atmospheric layers which differ by their different densities with altitudes. Let see how they impact on orbital decay:

Troposphere: This is lowest layer which extends 8 to 15 kilometers and here atmospheric density is very high compared to other layers. Hence drag forces are significantly very large which causes rapid orbital decay.

Stratosphere: The Stratosphere starts just above the Troposphere extending to 50 kilometers. Here density is relatively lower than that of Troposphere but still drag forces significantly influence on satellites.

Mesosphere: This layer starts from 50 kilometers and extended to 85 kilometers above. In this layer atmospheric density decreases but it can still contribute to orbital decay.

Thermosphere: Thermosphere starts just above the Mesosphere and extends to 600 kilometers. Atmospheric density in this area is relatively very low. Due to low density satellites in this layer experience minimal drag forces.

In presence of drag force, in order to simulate our numerical model it is necessary to use density as input during the time of simulation. For this we have to introduce a density function with altitude as independent variable. We assume that the atmospheric density can be described as an isothermal-barotropic atmospheric model with a fixed scale height. The temperature is assumed to be constant. As per this model the atmospheric density (ρ) as a function of altitude (h) can be expressed as [2][5]:

$$\rho(h) = \rho_0 e^{-\frac{h-h_0}{H}}, \quad (6)$$

where a reference atmospheric density ρ_0 is used with a reference altitude, h_0 and H is the atmospheric scale height.

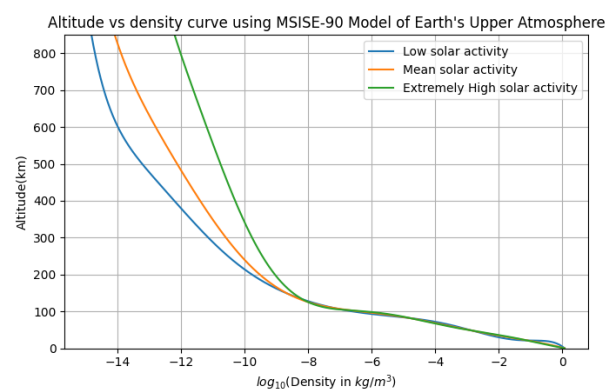


Fig 2: Variation of atmospheric density with altitude for low, mean and high solar activity as MSISE-90 model.

Drawbacks of density function:

While simulating numerical model starting from high altitude for lifetime prediction or any such measurements (i.e. simulation for long time) of a satellite, several density functions have to be used. While using different density functions to represent different atmospheric layers, a discontinuity can arise at the boundaries between these layers. This is the significant drawback in using density function.

To overcome the above mentioned problem we use fitted density data. We fit the densities of MSISE-90 model as a function of altitudes with a polynomial through curve fitting method.

Initially, we shall use the standard density function to calculate orbital decay rate but while doing 3D visualization for satellite life time prediction or re-entry time to the Earth surface or such applications we shall use fitted density. And we shall also compare the data obtained using these two methods. A variation of densities with different altitudes is shown in figure-2 for different solar activities as per MSISE-90 model. But we

shall use only mean solar activity data while doing numerical simulation.

(b) Quadratic drag:

In study of dynamics of orbital decay the concept of drag force becomes significant. This is nothing but a resistive force arising from the medium through which an object moves. We discuss here air drag (i.e. air resistance) as per our study of satellite orbital decay. Let us assume an object is moving with

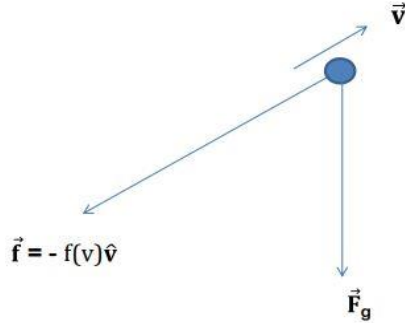


Fig 3: An object moving with velocity \vec{v} experiences two forces: Gravitational force (\vec{F}_g) and drag force due to air resistance, $\vec{f} = -f(v)\hat{v}$.

velocity \vec{v} through air medium. Obviously it will experience a drag force which is directed opposite to that of velocity vector (as in figure-3) can be expressed as [3]:

$$\vec{f} = -f(v)\hat{v}, \tag{7}$$

where $\hat{v} = \frac{\vec{v}}{|\vec{v}|}$ denotes the unit vector in the direction of \vec{v} and $f(v)$ is the magnitude of \vec{f} . The function $f(v)$ varies with v in a complicated way. However, it can be written with a good approximation that [3]:

$$f(v) = av + bv^2 = f_{linear} + f_{quadratic}. \tag{8}$$

For moving object is notably very small such as Millikan oil drop, linear drag can be applicable. While most of more obvious examples of objects such as baseballs, footballs, cannonballs, and of course satellite (in our case) experience pure quadratic drag, $f(v) = bv^2$. Now our focus should be on quadratic nature of drag force as we are discussing satellite motion within the Earth's atmosphere.

In Low Earth Orbit having relatively large atmospheric density, the effects of atmospheric drag is significantly high. Satellites moving in Low Earth Orbit, experience quadratic drag forces which opposes their motion and loses their energy which leads to ultimate cause of re-entry to the Earth surface. For a satellite orbiting in LEO the acceleration due to quadratic drag (a_d) can be expressed as [2]:

$$a_d = -\frac{1}{2} \frac{C_d A_s}{m_s} \rho(r) v_{rel}^2, \tag{9}$$

where C_d is the coefficient of drag, A_s is the projected area to the airflow, $\rho(r)$ is atmospheric density function, m_s is the mass of the satellite and \vec{v}_{rel} is the velocity of satellite relative to rotating atmosphere. The relative velocity (\vec{v}_{rel}) can be expressed as:

$$\vec{v}_{rel} = \vec{v}_s - (\vec{\omega}_A \times \vec{r}), \tag{10}$$

where \vec{v}_s is the satellite's original velocity vector, $\vec{\omega}_A$ is the atmospheric angular rotation velocity vector and \vec{r} be the radial vector of the satellite.

In this paper atmospheric rotational velocity is neglected. The drag coefficient C_d is a dimensionless quantity which depends on the satellite's shape, surface roughness and orientation to the airflow. It is determined experimentally or through computational simulations [4]. In the next subsection we shall incorporate this acceleration due to drag (a_d) term to determine the final equation of motion for a satellite orbiting in presence of atmospheric drag.

II.C Mathematical Formulation of Orbital Decay Model

In this subsection we formulate equation of motion of satellite in presence drag forces. Without atmospheric drag, considering circular orbit we obtain the equation of motion of a satellite from equation-4: $\frac{d^2\vec{r}}{dt^2} = -\frac{GM}{r^2}\hat{r} = -\frac{GM}{r^3}\vec{r}$.

To incorporate the atmospheric drag effect into the equation of motion, the acceleration due to drag (a_d) from equation-9 is added as follows:

$$\frac{d^2\vec{r}}{dt^2} = -\frac{GM}{r^3}\vec{r} - \frac{1}{2} \frac{C_d A_s}{m_s} \rho(r) v_s \vec{v}_s. \tag{11}$$

Here we assume $\vec{v}_{rel} = \vec{v}_s$ by neglecting atmospheric angular rotation velocity. The above equation can be splitted into a set of coupled second order differential equations in terms of x and y coordinate as given below:

$$\frac{d^2x}{dt^2} = -GM \frac{x}{(x^2+y^2)^{\frac{3}{2}}} - \frac{1}{2} \frac{C_d A_s}{m_s} \rho(r) \sqrt{(v_x^2 + v_y^2)} v_x, \tag{12}$$

$$\frac{d^2y}{dt^2} = -GM \frac{y}{(x^2+y^2)^{\frac{3}{2}}} - \frac{1}{2} \frac{C_d A_s}{m_s} \rho(r) \sqrt{(v_x^2 + v_y^2)} v_y. \tag{13}$$

Here we assume the motion of satellite in a plane, say xy plane. The above set of coupled 2nd order differential equations can be solved numerically. We use 4th order Runge Kutta method to solve these set of equations. Once we solve this we obtain instantaneous position components as a function of time i.e. $x = x(t)$ and $y = y(t)$ as well as velocity components as a function of time i.e. $v_x = v_x(t)$ and $v_y = v_y(t)$ of satellite. As drag force is applied to the equation of motion, at every instant of time satellite's radial distance i.e. altitude (h) changes with time. With changing altitude (h) the atmospheric density (ρ) also changes. And corresponding acceleration due to drag (a_d) updates with change in atmospheric density (ρ). In this way we numerically solve this problem. Solving these set of equations we can calculate several interesting decay parameters. In this paper, we have calculated some parameters such as radial decay (Δr) per revolution, change in time period (ΔT) and in 3D visualization section we have determined lifetime of satellite.

II.D An Analytical Approach to Calculate Decay Rate

In this subsection we derive analytically the change in radial distance and the change in orbital period of a satellite. In numerical section we shall verify our numerical data with respect to data determined by theoretical formula which will be derived in this section. But one thing is must have to be noted that this analytical formula is valid only for high altitude where atmospheric density is very low. We assume the motion of a satellite of mass m_s in a circular orbit of radius r , the total mechanical energy becomes $-\frac{GMm_s}{2r}$. The orbital

velocity (v_s) of satellite in circular orbit is calculated as follows:

$$v_s = \sqrt{\frac{GM}{r}}. \quad (14)$$

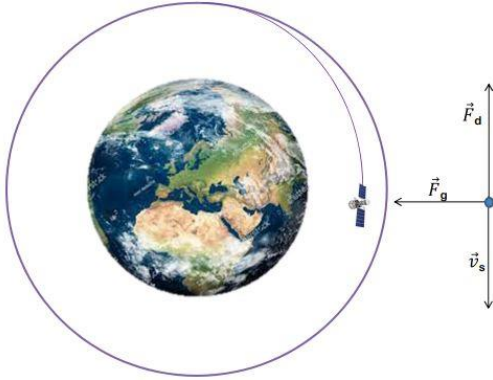


Fig 4: Schematic representation of satellite's orbital decay. This figure shows decrease in altitude due to atmospheric drag force \vec{F}_d .

In presence of atmospheric drag force, the mechanical energy losses over time. The loss of orbital energy is simply the work done by the drag force (\vec{F}_d) exerted on the satellite.

Let the satellite traverses an infinitesimal circular arc length ds spanned by some infinitesimal angle $d\theta$. The total energy loss turns out to be:

$$\Delta E = \int \vec{F}_d \cdot \vec{ds}. \quad (15)$$

Now we are going to calculate the energy loss per one full revolution. Integrating around for a full revolution we can express that:

$$\Delta E = \int_0^{2\pi} m_s a_d r d\theta. \quad (16)$$

Putting the value of a_d as well as ρ into equation-16 we obtain:

$$\Delta E = - \int_0^{2\pi} \frac{1}{2} A_s C_d \rho_0 e^{-\frac{h-h_0}{H}} v_s^2 r d\theta. \quad (17)$$

Using equation-14 we replace v_s^2 in equation-17 and therefore we find that:

$$\Delta E = - \int_0^{2\pi} \frac{1}{2} A_s C_d \rho_0 e^{-\frac{h-h_0}{H}} \frac{GM}{r} r d\theta. \quad (18)$$

We assume the radial distance change per revolution is very small and density remains constant over one orbital period as we considered the high altitude scenario which is typically 700 kilometers and above. Then the energy loss becomes:

$$\Delta E = -\pi G M A_s C_d \rho_0 e^{-\frac{h-h_0}{H}}. \quad (19)$$

We can calculate the energy loss by differentiating the total mechanical energy term ($-\frac{GMm_s}{2r}$) with respect to r , for Δr radial change as given below:

$$\Delta E = \Delta \left(-\frac{GMm_s}{2r} \right) = \frac{GMm_s}{2r^2} \Delta r. \quad (20)$$

On comparing equation-19 and 20 we can have the change in radial distance (Δr) that:

$$\Delta r = -\frac{2\pi A_s C_d}{m_s} r^2 \rho_0 e^{-\frac{h-h_0}{H}}. \quad (21)$$

The above formula of change in radial distance can be applied to verify the numerically obtained data of the same.

Now let us treat the change in orbital period (ΔT) analytically. From Kepler's third law as equation-5 we have $T^2 = \left(\frac{4\pi^2}{GM}\right) a^3$. As we already assumed circular orbit scenario of radius r , we therefore obtain by differentiating T^2 with respect to r that:

$$\Delta T = \frac{6\pi^2 r^2}{GM T} \Delta r. \quad (22)$$

Replacing Δr from equation-22 using equation-21 we have

$$\Delta T = -\frac{12\pi^3 A_s C_d}{GM m_s} \frac{r^4}{T} \rho_0 e^{-\frac{h-h_0}{H}}. \quad (23)$$

The above result of ΔT is the change in orbital period of satellite per one complete revolution.

III. NUMERICAL IMPLEMENTATION & RESULT ANALYSIS

In this section, we present the numerically obtained results and their analysis. The numerical implementation of LEO satellites orbital decay modeling is carried out in Python programming language. Numerical implementation enables us to examine the behavior of LEO satellites as they undergo orbital decay and evaluate the accuracy of our numerical model. The analysis of obtained results includes the examination of the satellite's altitude, velocity, change in radial distance and orbital period over time. The comparison of the obtained results to theoretical values and empirical data further facilitates the evaluation of model's accuracy. This analysis also offers valuable insights into the complex dynamics of LEO satellites orbital decay.

III.A Model Validation: A Primary Approach

Now before do the numerical calculations let's first check out this model's accuracy. In this subsection we validate our numerical model by comparing its results with established formula. We calculate numerically the time period of an orbiting satellite without atmospheric drag i.e. $C_d = 0$. And we compare this result with the theoretical formula (equation-5) obtained from Kepler's 3rd law i.e. law of harmonics. Our results are tabulated below.

TABLE 1: Time period of a moving satellite in a circular orbit around the Earth keeping drag coefficient, $C_d = 0$.

Satellite Mass (kg)	Altitude (km)	Numerical time period, ($T_{numerical}$) (seconds)	Theoretical time period ($T_{theoretical}$) (seconds)
900	700	5926.207011027913	5926.2070110227944
	710	5938.77051702598	5938.770517025938
	720	5951.342888671068	5951.342888671101
	730	5963.924119716043	5963.924119716057
	740	5976.514203926457	5976.514203926616
	750	5989.113135081809	5989.113135081734
	760	6001.720906973351	6001.720906973458

Table-1 presents a comparison between the values of time period of an orbiting satellite calculated by numerical method and theoretical formula. We observe that the two time periods are matching of the order of 10^{-10} seconds. This remarkable agreement serves as a valuable validation of our numerical model. Now we are going to apply air drag to our differential equation and calculate several decay parameters.

III.B Numerical Data Analysis

In LEO, the altitude of a satellite gradually decreases over time due to atmospheric drag. The analytical result does not hold good in low altitude where atmospheric density is very high. We calculate radial distance change per revolution at relatively high altitude, say $h=747.3489$ km. We compare our numerical results to the theoretical values. This comparison validates our numerical model and also provides confidence in the accuracy of our model. Before do that, let us now consider a satellite is moving in a circular orbit of radius, $r = h + R_e = 7125.3489$ km, where the radius of the Earth $R_e = 6378$ km. We use the atmospheric density function as [5]:

$$\rho = 3.614 \times 10^{-14} e^{-\frac{(h-700)}{88.667}}, \quad (24)$$

where the nominal atmospheric density has been taken as $\rho_0 = 3.614 \times 10^{-14} \text{ kg/m}^3$, the atmospheric scale height (H) and reference altitude (h_0) are taken as 88.667 km and 700 km respectively. We take satellite mass $m_s = 900$ kg and choose atmospheric drag coefficients $C_d = 2.0, 2.1, 2.2, 2.3$ and 2.4 respectively. Our results are given in tabulated form.

TABLE 2: Change of radial distance (Δr) for a fixed altitude (h) with different aerodynamic drag coefficients (C_d)

Satellite Mass (kg)	Altitude (km)	Atmospheric drag coefficient C_d	$\Delta r_{\text{numerical}}$ (m/rev)	$\Delta r_{\text{theoretical}}$ (m/rev)
900	747.3489	2.0	-0.0450588763	-0.0450580339
		2.1	-0.0473110266	-0.0473109356
		2.2	-0.049564627	-0.0495638373
		2.3	-0.0518162576	-0.051816739
		2.4	-0.0540686315	-0.0540696407

Table-2 as in the above demonstrates a comparison between numerical and theoretical results giving the values of change in radial distances. Theoretical values have been calculated using the analytical formula given in equation-21. We see our numerical results align (matching at least 5 decimal places) with results from the analytical formula making our model to be reliable.

TABLE 3: Change of orbital period (ΔT) for a fixed altitude (h) with different atmospheric drag coefficients (C_d)

Satellite Mass (kg)	Altitude (km)	Atmospheric drag coefficient C_d	$\Delta T_{\text{numerical}}$ (s/rev)	$\Delta T_{\text{theoretical}}$ (s/rev)
900	747.349	2.0	-5.67778×10^{-5}	-5.67776×10^{-5}
		2.1	-5.96166×10^{-5}	-5.96165×10^{-5}
		2.2	-6.24549×10^{-5}	-6.24554×10^{-5}
		2.3	-6.52944×10^{-5}	-6.52943×10^{-5}
		2.4	-6.81330×10^{-5}	-6.81332×10^{-5}

Table-3 compares the values of change in orbital period per revolution (ΔT) calculated using numerical method and theoretical formula. The comparison demonstrates up to the mark level of agreement between the two values of ΔT . The two values are matching up to 9 decimal places in s/rev units.

As we discussed earlier in subsection-II.B there are some drawbacks in using the density function. It is very much effective to fit the data of atmospheric density at different altitudes. We fit the densities from MSISE-90 model with a polynomial. Before using these fitted data, let us the check accuracy of fitting quality. Satellite mass and altitude are taken as 900 kg and 747.3489 km respectively.

In table-4 we present a comparison between the results using density function and fitted density in calculation of change in

radial distance. We observe that there is sufficient matching between two types of data. In spite of using two different types of density model, we are having the absolute difference (δr) is of the order of 1.5 mm to 1.8 mm in Δr data. This good agreement enables us to use the fitted density data.

TABLE 4: Comparison between the data of change of radial distance (Δr) using density function and fitted density

Atmospheric drag coefficient C_d	Δr (m/rev) with density function	Δr (m/rev) with fitted density	Absolute value of difference $\delta r = \Delta r_{\text{func.}} - \Delta r_{\text{fitted}} $ (m/rev)
2.0	-0.0450588763	-0.0465944633	0.001535587
2.1	-0.0473110266	-0.0489247618	0.0016137352
2.2	-0.049564627	-0.049564627	0.0016898597
2.3	-0.0518162576	-0.053583635	0.0017673774
2.4	-0.0540686315	-0.0559133347	0.0018447032

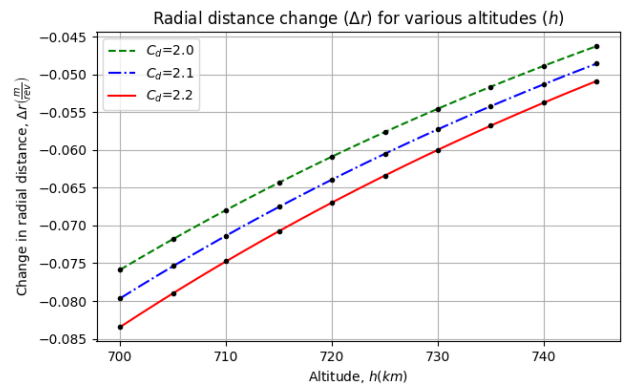


Fig 5: Change in radial distance Δr as a function of altitude h for a satellite of presented area $A_s = 3 \text{ m}^2$ and mass $m_s = 900$ kg in a circular orbit.

From figure-5 we observe the variation of radial distance change (Δr) with respect to altitude (h). We see that absolute value of Δr becomes smaller with increase in altitude which satisfies our theoretical idea. We also observe for increasing C_d values absolute Δr increases. The variation of Δr with altitude is not exactly linear rather there is some nonlinearity.

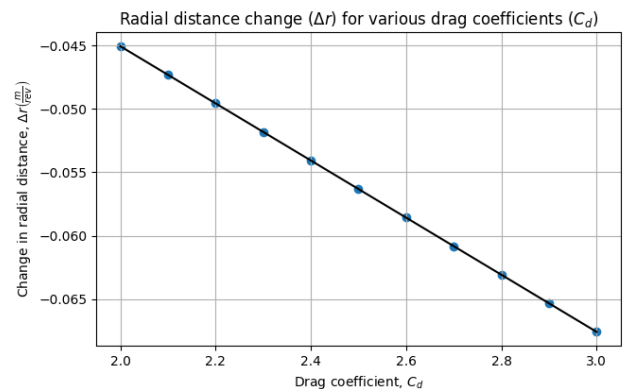


Fig 6: Radial distance change Δr for different atmospheric drag coefficients C_d with fixed altitude, $h = 747.3489$ km.

In figure-6 the graph of change in radial distance Δr as a function of drag coefficient C_d displays how Δr changes with C_d values. We observe that there is a linear variation of radial distance change Δr with drag coefficient C_d . This implies that there is a proportional relationship between the two variables.

When C_d increases the absolute value of Δr also increases i.e. satellite orbit decays rapidly.

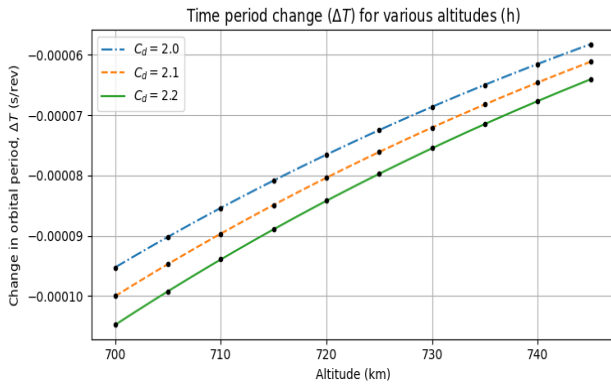


Fig 7: Change in time period per revolution (ΔT) as a function of altitude (h) for fixed drag coefficient (C_d).

Figure-7 points out how time period change per one complete revolution (ΔT) varies with altitude (h). There are smaller changes in absolute ΔT values for higher altitudes. On the other hand we observe with increasing C_d value absolute ΔT value increases i.e. time period change increases.

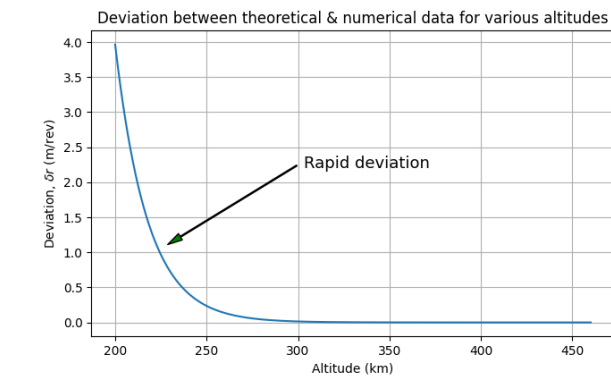


Fig 8: Deviation between theoretical and numerical data, δr (m/rev) in calculation of change in radial distance Δr as a function of altitude h (km).

In figure-8 we plot the deviation between theoretical and numerical data i.e. $\delta r = |\Delta r_{theoretical} - \Delta r_{numerical}|$ in calculation of change in radial distance (Δr) with varying altitudes in between the range of 200 to 460 kms. Here the atmospheric drag coefficient C_d is taken as 2.0. We observe that below 300 km there is a rapid increase in deviation and at 200 km δr turns out to be 3.957 m/rev. This indicates at lower altitudes the theoretical formula becomes less and less valid. As we already know at higher atmospheric density levels the theoretical formula does not hold good. This graph also reflects the same thing and hence proves our model's reliability.

Figure-10 provides a graphical representation of how speed of satellite changes with respect to its altitude over time. We observe this velocity variation with altitude from the height of 180 km above the Earth surface. At the beginning of the orbital decay process, the velocity of satellite is relatively constant and this corresponds to initial velocity which is typically $\sqrt{\frac{GM}{R_e+h}} = 7.802 \text{ km/s}$. During decay process as the satellite moves closer

to the Earth's surface, the gravitational force becomes more dominant. The graph exhibits at a certain point in the decay process the drag force acting upon the satellite becomes equal to the gravitational force, resulting the net force to be zero. From this point onward, the satellite's velocity remains relatively constant. This is terminal velocity as marked in the graph.

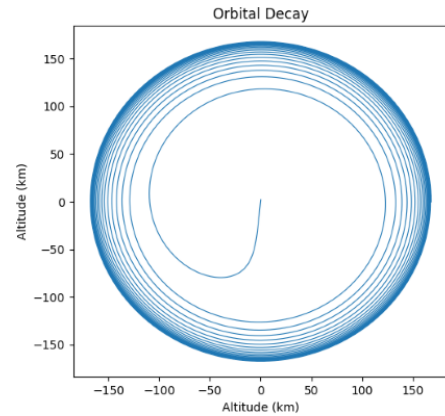


Fig 9: Polar graph depicting orbital decay from an altitude of 170 km.

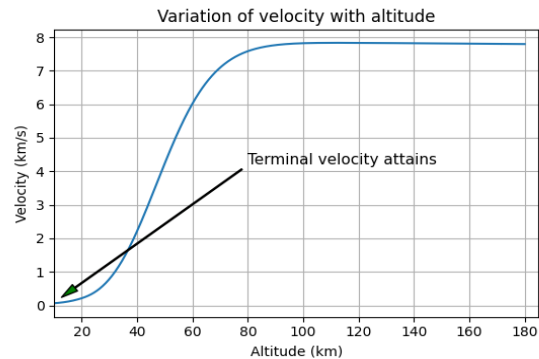


Fig 10: Velocity of satellite as a function of altitude with initial height 180 km.

III.C Validation of Numerical Model Against Experimental Data

In this subsection we validate our numerical model comparing the predictions of the model with empirical data from the ISS and Tiangong-1 missions. This is very crucial step in assessing the accuracy and reliability of the modelling approach.

International Space Station (ISS)

To validate our model against ISS experimental data, we first acquire relevant observational data from ISS mission records. We refer ISS trajectory data available on NASA's Open Data Portal as generated by the Trajectory Operations and Planning (TOPO) flight controllers at Johnson Space Centre [6]. The data file contains ISS mass, area of cross section (A_s) and drag coefficient (C_d) and those are given by 459023 kg, 1951 m^2 and 2.0 respectively. The time period of ISS is 92.9 minutes [7] and it orbits 15.5 times per day [8]. It usually it loses its altitude about 100 meters per day. For ISS orbital decay modelling, we use fitted atmospheric density data using MSISE-90 model. We conduct simulations for time duration of 24 hours at 1 km intervals between 426 and 418 km using provided data. The simulation results are given below in tabulated form.

From table-5 we observe that our numerical model generates reasonable data. The 100 meters/day decay rate and 92.9 minutes time period fall comfortably in the simulation results, ensures that the model works accurately.

Now let's see the orbital decay of ISS over time graphically at any particular altitude say 420 km. Then we shall observe ISS orbital decay over number of time periods at the same altitude in graphical representation.

TABLE 5: Decay rate and time period of ISS at different altitudes in between 426 and 418 km in intervals of 1 km.

Altitude (km)	Decay Rate (m/day)	Time Period (minutes)
426	-94.8406860084	93.0906137555
425	-96.4794844576	93.0700908189
424	-98.1486314731	93.0495693716
423	-99.8488000548	93.0290494132
422	-101.5806725882	93.0085309436
421	-103.3449432654	92.9880139623
420	-105.1423215223	92.9674984691
419	-106.9735194668	92.9469844635
418	-108.8392686583	92.9264719454

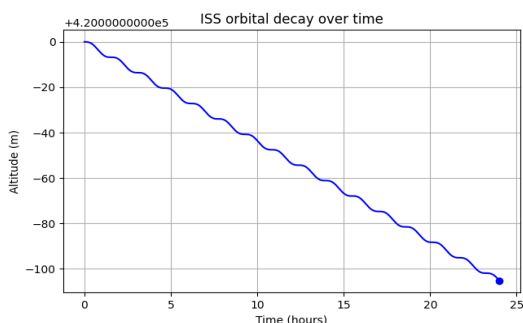


Fig 11: Decrease in altitude of ISS satellite over time at an altitude of 420 km.

Figure-11 displays how the altitude of ISS satellite decreases over time. In this figure we plot our numerically obtained data of ISS satellite at an altitude of 420 km where simulation is conducted for 24 hours. The decay in altitude for this time duration is already given in Table-5 which is nearly 105.1423 meters.

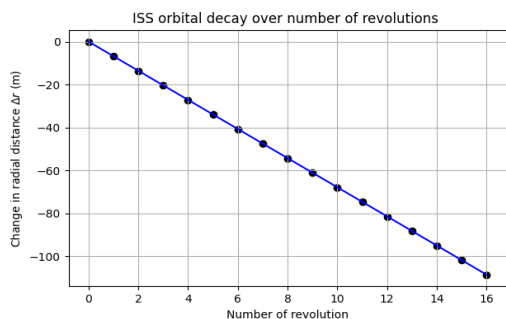


Fig 12: Radial distance change of ISS satellite with number of revolution at an altitude of 420 km.

Figure-12 depicts how orbit of ISS decays with number of revolutions. The graph is plotted using the simulation data of ISS satellite at an altitude of 420 km. The curve of radial decay with respect to number of revolutions is almost linear which indicates radial decay per revolution to be constant. As per mission records ISS orbits 15.5 times per day leads to 100 meters decay in altitude. Our numerical results reflect after 16th

revolution altitude reduces near about 108.68 meters (i.e. for 15.5th revolution radial decay turns out to be nearly 105 m).

Tiangong-1 satellite

Now we validate our numerical model using the uncontrolled reentry data of the Chinese space station Tiangong-1. According to Wikipedia, on 21 March 2016 the China Manned Space Agency (CMSA) announced that Tiangong-1 had officially ended its service. Tiangong-1 reentered the Earth's atmosphere over the central region of South Pacific on 2 April 2018 [9]. We use mass of Tiangong-1 as 8506 kg [10]. The following equation for atmospheric density is used [11],

$$\rho(h) = 6 \times 10^{-10} \exp\left(-\frac{h - 175}{H}\right) \quad (25)$$

where the reference density, $\rho_0 = 6 \times 10^{-10} \text{ kg/m}^3$ is used with a reference altitude, $h_0 = 175 \text{ km}$. The effective area of cross section ($A_{eff} = C_d A_s$) is taken as 41.8 m^2 with fixed scale height (H) 29.5 km [12].

During orbital decay Tiangong-1 stayed at an average altitude of 279 km on 17 January in 2018 [13]. We simulate our model at this altitude for time the duration from 17 January up to the end of 1 April of 2018. Now let's see our numerically obtained data graphically.

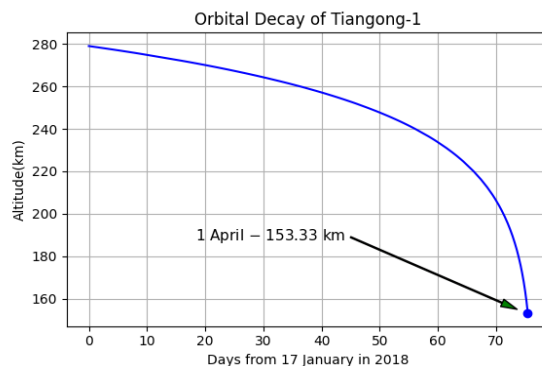


Fig 13: Reduction in altitude of Tiangong-1 satellite as a function of days in 2018 at an altitude of 279 km.

In figure-13 orbital decay of Tiangong-1 satellite is depicted graphically. Simulation is conducted at an altitude of 279 km with initial speed 7.738 km/s and time is counted from 17 January to end of 1 April of 2018. We observe that altitude reduces to 153.33 km on 1 April in 2018 as marked in the figure. In this figure, the radial decay curve exhibits a close alignment to the recorded decay trend of Tiangong-1 satellite, indicating the practical relevance and applicability of our modelling approach.

IV. VISUALIZATION

In this section we develop a 3D visualizing orbital decay model which can provide a dynamic representation of the satellite's trajectory and decay process. Our approach is to animate the model in 3D space, as well as pointing out of the latitude and longitude of the satellite's crashing location with given certain initial point. The whole task becomes very easy to perform by using vpython library in Python language.

We assume shape of the Earth to be spherical and origin of XYZ Cartesian coordinate system is at the centre of the Earth.

The Z-axis is the rotational axis and its positive direction points towards the North Pole whereas negative direction is towards the South Pole. The XY plane is the equatorial plane and the great circle which is located in this plane is the equator. The X-axis is in the direction of intersection of prime meridian & equator. The positive direction of X-axis points at zero degrees latitude and zero degrees longitude (0°N, 0°E). The positive Y-axis points towards zero degrees latitude and 90° east longitude.

So far we were solving equation of motion assuming motion of satellite in two dimensional XY plane i.e. equatorial plane which means the orbital plane of satellite assumed to be in equatorial plane. But this is not necessary to have orbital plane only in equatorial plane rather it may have oriented at a certain angle with equatorial plane. The desired orbital plane has to be chosen in such a way so that the initial position of satellite should be at any point on that plane. We can easily do it by coordinate transformation using rotation matrix. We first rotate XYZ frame about Z axis by longitude angle of satellite's initial position, say ϕ to produce $X'Y'Z'$ frame. Then again we rotate newly defined $X'Y'Z'$ frame about Y' axis by latitude angle of satellite's initial position, say λ to produce our desired $X''Y''Z''$ frame.

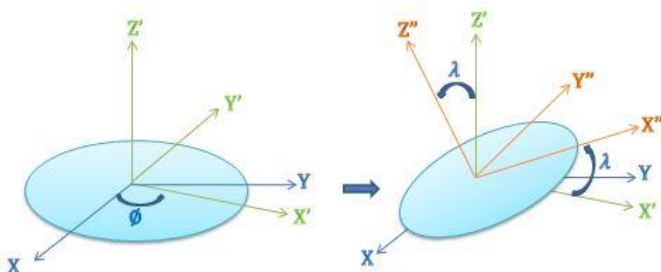


Fig 14: Representation of coordinate transformation from the coordinate system (XYZ) to a new coordinate system ($X''Y''Z''$).

The transformation equation has been given below.

$$\begin{bmatrix} x'' \\ y'' \\ z'' \end{bmatrix} = \begin{bmatrix} \cos \lambda & 0 & \sin \lambda \\ 0 & 1 & 0 \\ -\sin \lambda & 0 & \cos \lambda \end{bmatrix} \begin{bmatrix} \cos \phi & -\sin \phi & 0 \\ \sin \phi & \cos \phi & 0 \\ 0 & 0 & 1 \end{bmatrix} \begin{bmatrix} x \\ y \\ z \end{bmatrix} \quad (26)$$

The $X''Y''$ plane of the latest formed $X''Y''Z''$ frame is now the orbital plane of satellite and the great circle that is located in this plane is satellite's orbital path under circular orbit approximation. Satellite's initial latitude-longitude point is now on the X'' axis in the $X''Y''$ plane.

During simulation initial latitude (λ), longitude (ϕ) and altitude (h) of satellite are taken as input. Using this input data the respective orbital plane of satellite is set following the above discussed coordinate transformation method and then the satellite is projected in perpendicular to X'' axis along with the $X''Y''$ plane i.e. satellite's initial velocity vector becomes, $\vec{v}_s = v_0 \hat{y}''$. The set of coupled differential equations-12 & 13 can be solved in the $X''Y''$ plane of $X''Y''Z''$ frame and instantaneous position and velocity components can be transformed in terms of XYZ frame using equation-26. As the simulation continues, the altitude of satellite becomes zero after a certain time and the point at which the altitude becomes zero can be considered as the crashing point (or crashing location) of satellite. The crashing point in terms of XYZ Cartesian system can be transformed into Geographic coordinate system to find

geographic location (i.e. latitude and longitude) of crashing point.

There is another technique for the whole simulation procedure which can be done by using the vpython module directly. In this technique we directly solve the equation-11 in vpython environment. Initial position of satellite in terms of geographic coordinate system is taken as input. Then the position of satellite in geographic system is transformed into Cartesian system as the simulation runs in XYZ Cartesian system. The initial velocity vector $v_0 \hat{y}''$ is transformed in terms of XYZ frame using equation-26 and the satellite is projected with this velocity vector where v_0 is the magnitude of initial velocity which is nothing but $v_0 = \sqrt{\frac{GM}{R_e+h}}$. After running the simulation when magnitude of satellite's position vector minus radius of the Earth ($|\vec{R}| - R_e$) i.e. altitude (h) becomes zero, implying satellite's falling on the Earth's surface, the simulation stops. The final position of the satellite is noted as crashing point.

One thing is to be noted that generally decaying satellite burns up due to intense heating as a result of high friction between the satellite and air molecules in the atmosphere. If the satellite survives, it will eventually impact the Earth's surface and find out the respective location. Although the impact location is generally unpredictable due influence of many factors but our approach is the simplest one under certain approximations.

We already said earlier that we assume spherical shape of the Earth and the transformation equations between Cartesian and Geographic coordinate system are easily be written as follows:

$$\phi = a \tan 2 \left(\frac{y}{x} \right), \quad (27)$$

$$\lambda = \tan^{-1} \left(\frac{z}{\sqrt{x^2+y^2}} \right), \quad (28)$$

$$h = \sqrt{x^2 + y^2 + z^2} - R_e, \quad (29)$$

as we assumed λ , ϕ and h as latitude, longitude and altitude respectively. Here $a \tan 2$ implies four quadrant arc tangent.

We perform our numerical simulation using vpython module in Python language. To simulate our 3D model we use fitted density data using MSISE-90 model. We take the satellite's mass $m_s = 900$ kg, presented area $A_s = 3$ m² and atmospheric drag coefficient $C_d = 2.0$. The initial latitude, longitude and altitude are taken as 45.965°N, 63.305°E and 160 kilometers respectively.

Some snapshots of the visualization window are given here which were captured during running simulation.

The figure-15 shows a snapshot captured during the animation of satellite motion under drag with some initial conditions which are already mentioned. At a specific instant of simulation time 73 minutes, the satellite's orbital trajectory is depicted and illustrated other orbital parameters. At that instant, the satellite's latitude, longitude, altitude and speed are 20.916° N, 5.009° W, 157.83144 km and 7.80957 km/s respectively. The inclination angle of the orbital plane with equatorial plane becomes 45.97 degrees.

Now let's see at after how much time and at which location the satellite crashes under given initial conditions. Next we point out that crashing location in a Google map.

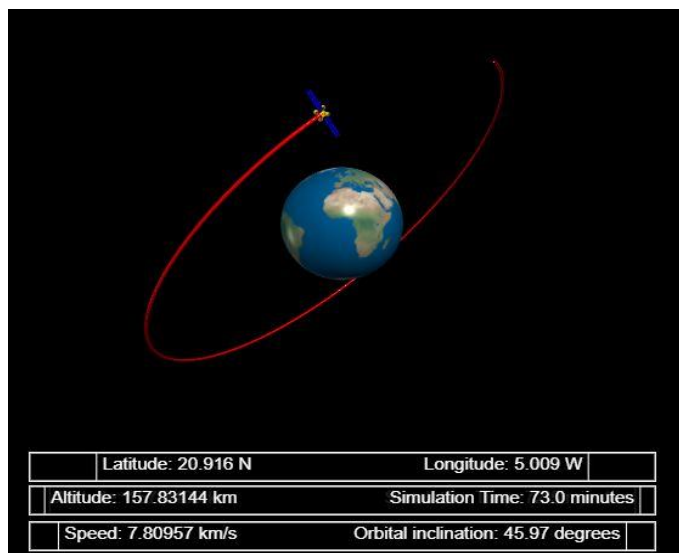


Fig 15: A snapshot of animated satellite motion under atmospheric drag at the simulation time of 73 minutes.

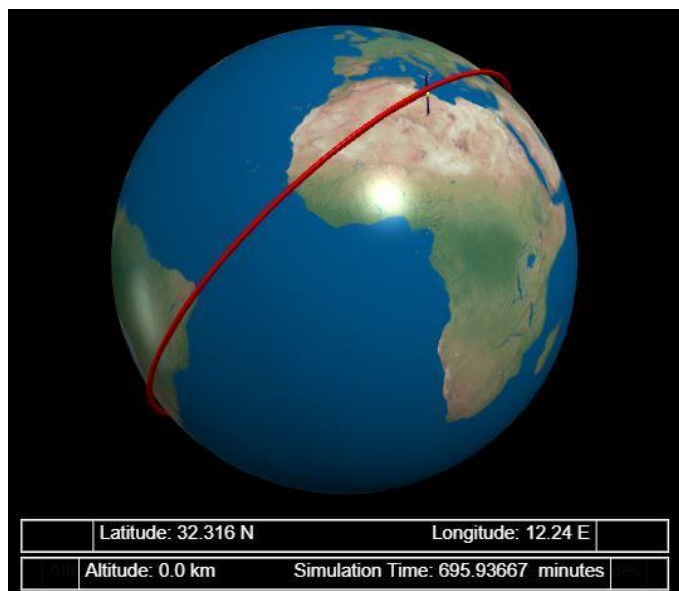


Fig 16: A snapshot of visualization widow of satellite motion captured at the end of the simulation.

Figure-16 offers a snapshot captured at the end of simulation when altitude becomes zero. This figure shows that after the time of 695.93667 minutes the satellite falls on Earth's surface i.e. crashes. The latitude and longitude of the crashing location are detected as 32.316° N and 12.24° E respectively.

The figure-17 points out the satellite's crashing location with a red colored marker in a portion of Google map. As we see on the map, an area south of Sabratha (also called Sabratabh) city of Libya on the shore of the Mediterranean Sea is being detected as the satellite's crashing location.

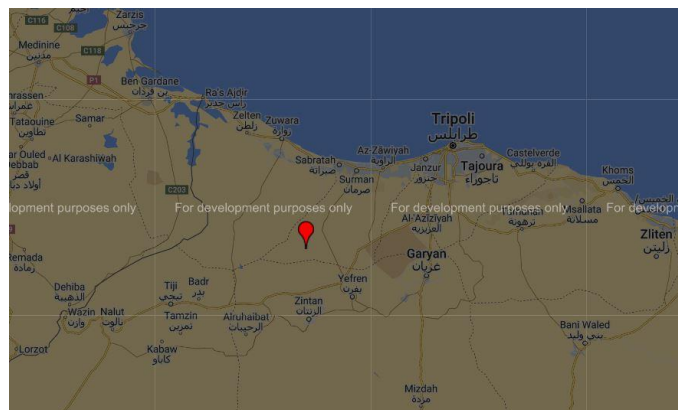


Fig 17: A portion of Google map where the satellite's crashing location is pointed out with a red marker.

The 3D visualization has not only presented a visual representation of orbital decay scenarios but also illuminated bridging the gap between mathematical calculation and observation. We have some realized the real world events in context of orbital decay of LEO satellites.

V. CONCLUSION

In this article, a general numerical solution to the orbital motion of a LEO satellite under atmospheric drag has been presented. At relatively high altitude (~700 kilometers) the method is applied to circular orbit. In presence of atmospheric drag the motion remains very close to circular one and the method could be applied to elliptical orbit with low eccentricity without difficulty. The set of time dependent coupled second order differential equations have been solved by RK4 method to find the instantaneous position $\vec{r}(t)$ and velocity $\vec{v}(t)$ in orbital plane of the satellite under the atmospheric drag at different altitudes starting from typically 700 kilometers.

On implementation of this model we gained valuable insights in the dynamics of orbital decay process. We have numerically calculated some decay parameters such as change in radial distance (Δr) and change in orbital period (ΔT) per revolution and validated the numerical results against analytical formula for relatively high altitudes.

We have presented graphically that how rapid decay occurs in low altitudes. We have also presented that how analytical results deviate from numerical ones in low altitudes. For assessing more accuracy of our model we have calculated decay rate and time period of ISS satellite and validated our numerical data to observational ones. We have also validated our numerical model using uncontrolled re-entry data of Tiangong-1 satellite. Furthermore, we have presented a 3D visualization to provide an immersive and intuitive representation of the satellite's trajectory. The visualization allowed for a dynamic exploration of orbital decay over time, highlighting the instantaneous geographic location and speed of satellite as well as pointing out the crashing location.

However, there are certain limitations to consider. In our numerical model we have neglected non-spherical potential of Earth, rotation of Earth, atmospheric velocity and other perturbative effects on satellite motion. This may impact the model's accuracy in specific scenarios.

Future research in this area can build upon the foundations established in this article. Refining the model to additional work such as to use rotating frame of reference, incorporate the effects of the Earth's oblateness and use more accurate atmospheric models will enhance farther our model's accuracy and practical utility.

ACKNOWLEDGEMENT

This work was done as M.Sc. (Physics) project provided by Barasat Government College. I would like to thank to my supervisor Prof. Uttam Sinha Mahapatra for his valuable guidance, individual care and encouraging words throughout the entire project work. I acknowledge my gratitude to the Dept. of Physics, Barasat Government College for providing me suitable environment to carry out this project work.

REFERENCES

[1] <http://www.braeunig.us/space/atmos.htm>

- [2] J De Lafontaine and S C Garg, Proc. Indian Acad. Sci (Engg.Sci) Vol 5, september 1982, pp. 197-258.
- [3] John R. Taylor, Classical Mechanics, University Science Books, January 1, 2005.
- [4] Jacob Bullard, Master thesis on Satellite drag analysis using direct simulation Monte Carlo (DSMC), University of Hertfordshire (2018).
- [5] Vallado DA Fundamentals of Astrodynamics and Applications, 3rd Edition Springer, Berlin (2007).
- [6] NASA Open Data Portal - Trajectory Operations and Planning (TOPO), ISS_COORDS_2022-01-03 Public Distribution File-
https://data.nasa.gov/Space-Science/ISS_COORDS_2022-01-03/ffwr-gv9k
- [7] <https://karhukoti.com/webtracker?s=25544>
- [8] <https://www.heavens-above.com/orbit.aspx?satid=25544>
- [9] http://en.cmse.gov.cn/art/2018/4/2/art_1763_32429.html
- [10] <https://nssdc.gsfc.nasa.gov/nmc/spacecraft/display.action?id=2011-053A>
- [11] J. Kennewell, "Satellite orbital decay calculations," Australian Space Weather Agency, 111 (1999).
- [12] Carlos Chaparro, Andrea Ferrogliia, Miguel C. N. Fiolhais, Luis Gonzalez-Urbina, Tomasz Milewski, "Orbital decay in the classroom", City University of New York (CUNY), 2023.
- [13] http://en.cmse.gov.cn/announcement/201801/t20180116_44684.html